Volume 2, Issue 1

Innovation Series Quarterly

https://journal.academicapress.org/aps/index.php/isq

Research Article

Tropical Climate Fire Hazard Index (FHI)

Afiqah Zahidah Anwarzaini[1], and Nazirah Md Tarmizi[2*]

[1,2] Faculty of Built Environment, Universiti Teknologi MARA, Perlis Branch, Arau Campus, Malaysia; 2023227964@student.uitm.edu.my, nazir230@uitm.edu.my

* Correspondence: nazir230@uitm.edu.my; +60 10-911 6170.

Keywords:
Wildfire
Fire Hazard Index
Geospatial Analysis
Spectral Indices
Fire Mitigation

Abstract: *Wildfire incidents have become an alarming phenomenon that threatens the ecology, economy, and public safety. Thus, this research aimed to develop a Fire Hazard Index using LST, NDVI, NDMI, NDWI, NDDI, and NBR to suit the tropical climate region. The spectral indices were extracted from the Landsat 8 image, and the MLR was applied to obtain the correlation coefficients. The results show that the index was statistically significant and describing 71% (R^2 = 0.71) of the variation in the data. Geospatial technologies and spectral data applied in this innovation would help authorities to optimize resource allocation and perform controlled burns.*

1. INTRODUCTION

Wildfires are being recognized as one of the most catastrophic natural disasters and significantly influence global ecosystems, the resilience of human cultures and economy, as well as the political stability. In recent decades, wildfires have increased in frequency, intensity, and duration globally. This is mostly due to the combined effects of climate change, prolonged droughts, and alterations in land utilization (Chew et al., 2022). Previously, wildfire occurrence was mainly caused by human activities. Since late year 2019, elevated temperatures, strong winds, and low relative humidity promoted circumstances conducive to high-intensity wildfire behaviour (Thangavel et al., 2023). Arid conditions and elevated temperatures due to climate change primarily affect the deteriorated regions that are susceptible to fire. Wildfires, including unintended forest fires and bushfires, are measured using various indices such as fuel moisture content, relative humidity, temperature, and precipitation (Bandara et al., 2023). This catastrophic phenomenon has become a global annual incident.

Most of the studies conducted in Malaysia have utilized spectral indices to monitor wildfire occurrence; however, the studies generally focused on assessing the severity of burning after a fire occurred. There are still deficiencies in studies related to the generation of the fire hazard index using multispectral indices. For that reason, this study aimed to drive a Fire Hazard Index (FHI) for Perlis state using LST, NDVI, NDMI, NDWI, NDDI, and NBR through geospatial analysis, emphasizing the following objectives: to determine the spectral indices in Perlis using the Landsat 8 OLI/TIRS image, and to identify the correlation coefficient using the Multiple Linear Regression (MLR) method. However, this study only discusses the environmental conditions in Perlis state during the dry season,

which typically takes place in March, and does not take into account other months in that particular year.

2. LITERATURE REVIEW

2.1 Wildfire Issues in Tropical Climate Countries

Southeast Asia (SEA) countries, which predominantly experience a tropical climate had witnessed a few wildfire occurrences in the past decades. In the dry season, the incidence of wildfires in Thailand's protected forest regions was 4,207, 4,982, and 6,685 in the years 2014, 2015, and 2016, respectively (Burapapol & Nagasawa, 2016). Meanwhile, Brunei Darussalam suffered an 80% rise in forest fires, especially from 2007 to 2016 (Zahran et al., 2020). In Indonesia, approximately 135,000 Ha of Indonesian forests were damaged by wildfire in the year 2019, with the largest cases reported in the South Sumatra region (Rendana et al., 2023). Besides, between 2009 and 2018, Vietnam encountered 4,571 forest fires, destroying almost 22,000 acres of forest, with a high in the year 2010, where 6,723 hectares were destroyed (Nguyen & Tong, 2023).

Likewise, Malaysia also encounters several catastrophic wildfires that commonly occur in forested region especially during the dry season. From 1992 to 1998, Malaysia reported a total of 1,232 forest fire incidents (Jamaruppin et al., 2016). In Sabah, the occurrence of forest fires affects an area of around one million hectares, due to the El Niño phenomenon (Fisal et al., 2017). Though the majority of fires in Peninsular Malaysia were classified as small-scale, affecting areas less than 100 hectares, the increase in frequency and intensity due to hot and dry weather is still worrying (Chew et al., 2023). Therefore, frequent and rapid monitoring of the high-risk areas should be practiced. Apart from SEA countries, the other countries that experienced the tropical climate are African countries, South and Central America countries, and Pacific Island countries.

2.2 Spectral Indices Used in Wildfire Monitoring

Mapping of wildfire hazard zones is important for post-fire management and mitigation action, as it enables the identification of hotspots within a specified region. Spectral analysis has been widely adopted in monitoring applications, such as vegetation health, soil properties, and water levels. Wildfire occurrence can also be monitored using a combination of several spectral indices extracted from satellite images. This spectral modelling technique identifies hotspots efficiently where elevated temperatures coincide with low moisture levels, indicating areas most susceptible to major fires.

2.2.1 Land Surface Temperature (LST)

Land Surface Temperature (LST) indicates the temperature of the Earth's surface. Thermal bands 10 of Landsat 8 OLI/TIRS were utilized, and the computation was conducted using the mono-window method. According to Moisa et al. (2023), the steps involved are the conversion of digital numbers to radiance, the conversion of radiance to brightness temperature, the determination of land vegetation proportion using NDVI, the determination of land surface emissivity, and the determination of LST using brightness temperature and corrected emissivity. The final formula used to derive LST is as follows:

$$LST = \left[\frac{BT}{1 + (W \times BT/P)\ln\varepsilon}\right] - 273.15$$

Where LST is the land surface temperature in Celsius, BT is the Brightness Temperature, W is the wavelength of emitted radiance constant, P is the constant value which is equal to 1.438×10−2 m K, and ε is the emissivity. Climate-related factors, particularly average and maximum temperatures, were utilized in the estimation of forest fire risk (Nguyen & Tong, 2023) since a significant temperature rise is related to an elevated possibility of wildfire occurrence, especially in bushland and vegetated areas.

2.2.2 Normalized Difference Vegetation Index (NDVI)

The Normalized Difference Vegetation Index (NDVI) is an indicator used to evaluate the vegetation condition, whether healthy or unhealthy. The NDVI value ranges from +1, indicating healthy and hydrated vegetation, to -1, indicating unhealthy vegetation or non-vegetative areas (Artikanur et al., 2022). The NDVI was derived from Landsat 8 OLI/TIRS near infrared (NIR) and red bands, represented by bands 5 and 4, respectively. As suggested by Moisa et al. (2023), the formula used to calculate NDVI is:

$$NDVI = \frac{\rho_{NIR} - \rho_R}{\rho_{NIR} + \rho_R}$$

Where ρ_{NIR} is the spectral reflectance band for near infrared, which is band 5, and ρ_R is the spectral reflectance band for red, which is band 4. This index is essential in wildfire monitoring as it gives an insight of fuel condition of different vegetation types.

2.2.3 Normalized Difference Moisture Index (NDMI)

Normalized Difference Moisture Index (NDMI) represents the moisture content of soil and vegetation. The NDMI value ranges from -1, indicating high water stress, to +1, indicating very low or no water stress (Rendana et al., 2023). The NDMI was extracted from Landsat 8 OLI/TIRS short-wave infrared and near infrared bands, represented by band 6 and band 5, respectively. According to Rendana et al. (2023), the formula used to calculate NDMI is shown below:

$$NDMI = \frac{\rho_{NIR} - \rho_{SWIR}}{\rho_{NIR} + \rho_{SWIR}}$$

Where ρ_{NIR} is the spectral reflectance band for near infrared and ρ_{SWIR} is the spectral reflectance band for short-wave infrared. This index is crucial in assessing the probability of wildfire occurrence, as dry vegetation is highly flammable and dry soil can lengthen the duration of the fires.

2.2.4 Normalized Difference Water Index (NDWI)

Normalized Difference Water Index (NDWI) is an index used to distinguish water bodies from other features in a particular area. The NDMI value ranges from -1, denoting no water, to +1, denotes as presence of water bodies (Artikanur et al., 2022). Landsat 8 OLI/TIRS green and near infrared bands were used to derive the NDMI values, and the formula used is suggested by Moisa et al. (2023):

$$NDWI = \frac{\rho_{GREEN} - \rho_{NIR}}{\rho_{GREEN} + \rho_{NIR}}$$

Where ρ_{GREEN} is the spectral reflectance band for green, which corresponds to band 3 and ρ_{NIR} is a spectral reflectance band near infrared, which corresponds to band 5. NDWI that usually used to distinguish water bodies, also poses a slight impact on the temperature changes, because the increase in surface temperature eventually decreases the water level in small water bodies such as lakes, reservoirs, and streams.

2.2.5 Normalized Difference Drought Index (NDDI)

The Normalized Difference Drought Index (NDDI) indicates the dryness severity across all features on the surface. The NDDI value generally ranges from -1, indicating low drought severity, to +1, indicating high drought severity (Artikanur et al., 2022). The NDDI was calculated using previously derived NDVI and NDWI, and according to Nguyen & Tong (2023), the formula was:

$$NDDI = \frac{NDVI - NDWI}{NDVI + NDWI}$$

2.2.6 Normalized Burned Ratio (NBR)

Normalized Burned Ratio (NBR) is an index used to measure the severity and perimeter of the burned areas. The NBR value also ranges from -1, indicating burned areas, to +1, indicating unburned areas (Anucharan et al., 2025). The NBR was derived from a Landsat 8 OLI/TIRS image using near infrared and short-wave infrared 2, represented by bands 5 and 7, respectively. The formula used to calculate NBR was suggested by Anucharan et al. (2025), and the equation is shown below:

$$NBR = \frac{\rho_{NIR} - \rho_{SWIR2}}{\rho_{NIR} + \rho_{SWIR2}}$$

Where ρ_{NIR} is the spectral reflectance band infrared, which is band 5, and ρ_{SWIR2} is the spectral reflectance band short-wave infrared, which corresponds to band 7. NBR is highly sensitive to the black and grey colour spectrum, thus making it useful in detecting dehydrated soil and vegetation before the wildfire occurrence.

2.3 Wildfire Hazard Modelling Using Multiple Linear Regression (MLR)

Multiple Linear Regression is a statistical analysis that is able to model the interaction of multiple parameters to forecast various conditions, such as retail business forecasting, insurance pricing, and fire prediction. The main advantage of applying MLR to model wildfire hazard zones is that it organizes variables according to their respective impact on the model, emphasizing their significance in understanding wildfire occurrence (Oliveira et al., 2012). In a study by Liu & Zhang (2015), the fire rating prediction model using MLR was derived as:

$$\hat{y} = -5.066 - 0.0643x_1 + 0.1446x_2 + 0.0871x_3 + 1.2271x_4$$

Where $\hat{y}$ is the fire rating model, and x_1, x_2, x_3, and x_4 are the selected variables. The numbers before each variable are the correlation coefficients calculated using the MLR technique. A wildfire hazard zonation map can be created by integrating the layers of spectral indices based on their respective coefficients into the model.

3. METHODOLOGY

This study utilized remote sensing data and GIS software to derive a Fire Hazard Index (FHI) for Perlis state. The procedure involves data acquisition and pre-processing, derivation of each index, correlation analysis using MLR, and the derivation of FHI based on the correlation analysis. The datasets used in this study are the Landsat 8 OLI/TIRS image retrieved in March 2024. ArcMap 10.5 software will be utilized to process the data. The software facilitates the MLR process through the Ordinary Least Squares (OLS) tools.

3.1 Study Area

This study was conducted at Perlis, Malaysia, situated between latitude 6°30' N and longitude 100°15' E. The predominant topography consisted of semi-deciduous forest and agricultural fields. Although Perlis is the smallest state in Malaysia, the state's average temperature is 0.17% higher than the average temperature of Malaysia, and the warmest and driest month was observed in February and March (The Global Historical Weather and Climate Data). Figure 1 illustrates the map of the studied area.

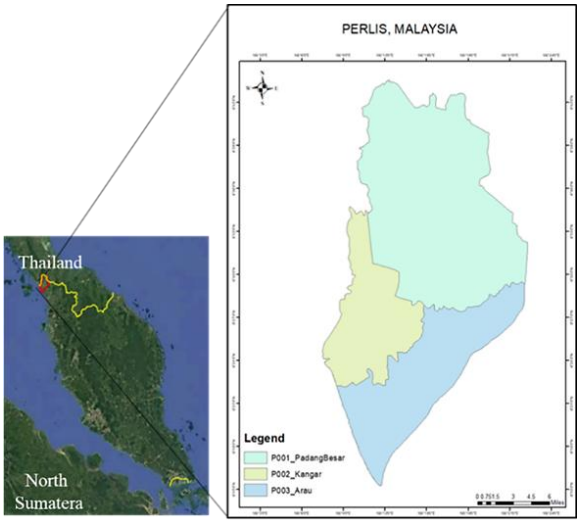

Figure 1. Map of the studied area.

3.2 Data Acquisition and Pre-Processing

The Landsat 8 OLI/TIRS image was obtained from the USGS Earth Explorer, an open-source database. The chosen spectral bands, which are bands 3, 4, 5, 6, 7, and 10, were downloaded in Geo-TIFF format. The satellite image was particularly selected in March 2024, with cloud cover less than 20%. The image was pre-processed to correct the radiometric and geometric errors using ArcMap 10.5 software. To ensure the data overlapped correctly, the data was projected to a global coordinate system, which is WGS84, using the Projection and Transformation tool.

3.3 The Derivation of the Spectral Indices

The spectral indices were derived from the corrected bands of the Landsat 8 OLI/TIRS image using the Raster Calculator tool in ArcMap 10.5 software. In accordance with Moisa et al. (2023), the LST was derived using a mono-window method. Table 1 presents the formulas involved in the derivation of LST, while Table 2 presents the formulas used to derive NDVI, NDMI, NDWI, NDDI, and NBR as suggested by Anucharan et al. (2025), Moisa et al. (2023), Nguyen & Tong (2023), and Rendana et al. (2023).

Table 1. The formulas used to derive LST using the mono-window method

Steps	Formulation used	Description
i.	The conversion of a digital number to radiance $L_\lambda = M_L \times Q_{cal} + A_L$	L_λ is the top of atmosphere radiance M_L is the band 10 radiance multiplicative constant Q_{cal} is the corresponding band 10 A_L is the band 10 radiance additive constant
ii.	The conversion of radiance to brightness temperature $BT = \frac{K2}{\ln\left(\frac{K1}{L_\lambda} + 1\right)}$	BT is the brightness temperature in Kelvin $K2$ is the K2 band 10 thermal conversion constant $K1$ is the K1 band 10 thermal conversion constant L_λ is the top of atmosphere radiance
iii.	The determination of vegetation proportion using NDVI $P_v = \left(\frac{NDVI - NDVI_{min}}{NDVI_{max} - NDVI_{min}}\right)^2$	P_v is the vegetation proportion $NDVI$ is the corresponding NDVI raster $NDVI_{min}$ is the minimum value of the NDVI

		$NDVI_{max}$ is the maximum value of the NDVI
iv.	The determination of land surface emissivity $\varepsilon = 0.004 \times P_v + 0.986$	ε is the land surface emissivity P_v is the vegetation proportion
v.	The determination of LST using brightness temperature and corrected emissivity $LST = \left[\frac{BT}{1 + (W \times BT/P)\ln\varepsilon}\right] - 273.15$	LST is the land surface temperature in Celsius BT is the brightness temperature W is the wavelength of emitted radiance constant P is the constant value which is equal to 1.438×10−2 m K ε is the land surface emissivity

Table 2. The formulas used to derive NDVI, NDMI, NDWI, NDDI, and NBR

No.	Formulation used	Description
i.	$NDVI = \frac{\rho_{NIR} - \rho_R}{\rho_{NIR} + \rho_R}$	$NDVI$ is the normalized difference vegetation index ρ_{NIR} is the near infrared band, which corresponds to band 5 ρ_R is the red band, which corresponds to band 4
ii.	$NDMI = \frac{\rho_{NIR} - \rho_{SWIR}}{\rho_{NIR} + \rho_{SWIR}}$	$NDMI$ is the normalized difference moisture index ρ_{NIR} is the near infrared band, which corresponds to band 5 ρ_{SWIR} is the short-wave infrared band, which corresponds to band 6
iii.	$NDWI = \frac{\rho_{GREEN} - \rho_{NIR}}{\rho_{GREEN} + \rho_{NIR}}$	$NDWI$ is the normalized difference water index ρ_{GREEN} is the green band, which corresponds to band 3 ρ_{NIR} is the near infrared band, which corresponds to band 5
iv.	$NDDI = \frac{NDVI - NDWI}{NDVI + NDWI}$	$NDDI$ is the normalized difference drought index $NDVI$ is the normalized difference vegetation index $NDWI$ is the normalized difference water index
v.	$NBR = \frac{\rho_{NIR} - \rho_{SWIR2}}{\rho_{NIR} + \rho_{SWIR2}}$	NBR is the normalized burned ratio ρ_{NIR} is the near infrared band, which corresponds to band 5 ρ_{SWIR2} corresponds to band 7

3.4 The Correlation Analysis Using MLR and the Derivation of FHI

The values of the derived spectral indices were extracted and combined into one feature layer to facilitate the process of statistical analysis using MLR. Before executing data extraction, random sample points were generated covering the whole studied area. Then, the Extract Multi Values to Points tool was used to extract the values of the calculated spectral indices to the weighted point data. The calculation of correlation coefficients was performed using the Ordinary Least Squares (OLS) tool. The report was generated, and the correlation coefficients for each spectral index were obtained. The calculated correlation coefficients of the spectral indices and the intercept constant were used to construct the Fire Hazard Index (FHI) for Perlis state. Figure 2 illustrates the overall methodology workflow for this study.

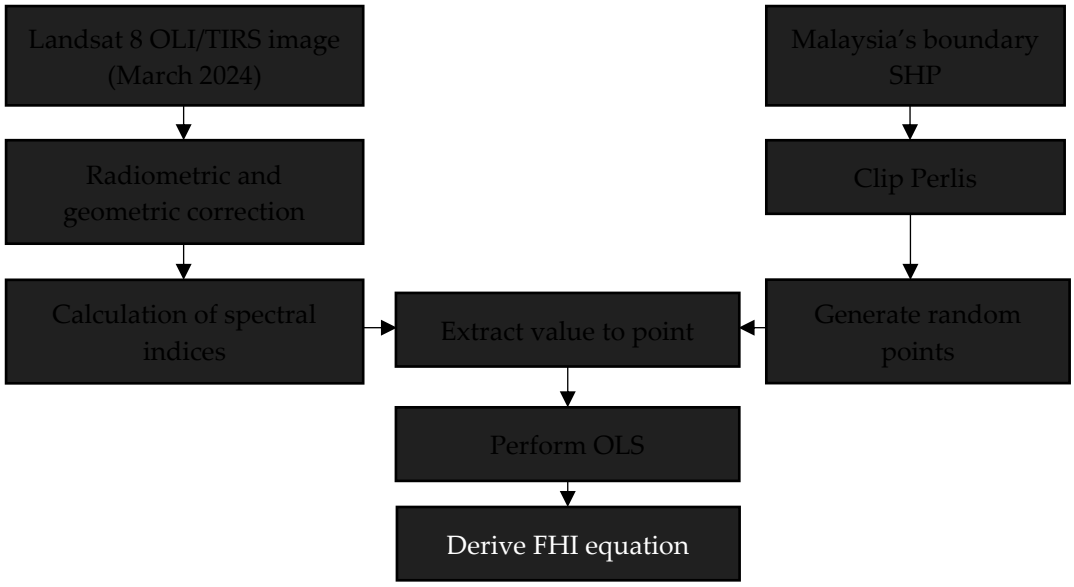

Figure 2. The general workflow of the proposed study

4. FINDINGS

The increase in wildfire occurrence frequency has demanded a framework to monitor and identify hotspots of the incidents. Such a framework assists local authorities in preventing hazardous activities such as burning crop residue or operating heavy-duty machinery in high-hazard areas, especially during the hot and dry season. The correlation between the multispectral indices and wildfire occurrence in Perlis obtained from the OLS processing is presented in Table 3. As presented in the table, the FHI model was statistically significant and describing 71% (R^2 = 0.71) of the variation in the data. The high R^2 value indicates that the chosen spectral indices fit well in the generated model. The p-value < 0.05 indicates that the predictor variable is likely to exert an influence on the dependent variable since the correlation is statistically significant. The correlation coefficient value for each spectral index is illustrated in Figure 3.

Table 3. Result of the correlation model between multispectral indices and wildfire occurrence

Variable	R^2	Standard error	p-value
FHI	0.717	1.094	0.0001

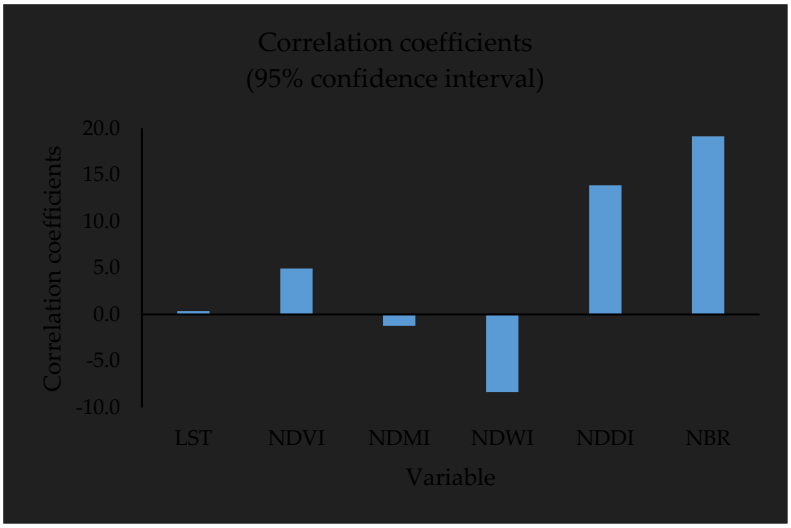

Figure 3. The standardized coefficients of the chosen spectral indices

From the figure, it can be seen that NDMI and NDWI were negatively correlated, while the other indices were positively correlated with the wildfire occurrence. The highest coefficient was observed in NBR, followed by NDDI, with the value approximately 20 and 15, respectively, indicating that these indices are the most significant influential factors in the model. Contrariwise, LST has the lowest coefficient, followed by NDMI with the value nearest to 0, indicating that these indices are the least significant in the model. The generated FHI equation from the calculated intercept and coefficients is demonstrated in Equation 1.

$$\mathrm{FHI} = -9.460 + 0.366x_1 + 4.946x_2 - 1.218x_3 - 8.330x_4 + 13.876x_5 + 19.122x_6$$

Equation 1. The FHI equation to identify the wildfire hazard zone in Perlis

Where the x_1 is LST, x_2 is NDVI, x_3 is NDMI, x_4 is NDWI, x_5 is NDDI, and x_6 is NBR.

5. DISCUSSION

The findings of this study demonstrate that multispectral indices derived from satellite data are particularly effective indicators of fire risk, due to their ability to reflect the surface temperature, the state of health of the vegetation, and the moisture level. Figure 3 presents the correlation coefficients of the spectral indices, and based on the coefficients' value, the most significant influential factors are the NBR, followed by NDDI. Contrariwise, the LST was the least significant in the model. This finding suggests that LST has reached its absolute threshold during the prolonged hot and dry weather. Since this study utilized satellite images retrieved in March, which marks the peak of the hot and dry season, it can be assumed that the vegetation was critically dehydrated. LST is known as a significant factor in the dehydration of fuels; however, in areas that are extremely dry, other factors, such as NDDI and NBR, hold greater importance in assessing the fire risk. This view is supported by Liu & Zhang (2015), who conducted a study during the prolonged dry season, and revealed that the wind speed is the most significant factor, with a coefficient value of 12.21, while maximum temperature has the lowest coefficient value of 0.064. Besides, a forest fire risk prediction map (FFRPM) equation constructed by Nguyen & Tong (2023) also demonstrated that NDDI holds the highest weighting value of 0.30, compared to LST with 0.15. Since the NBR is the strongest influential factor, the FHI is suitable to be used after a fire occurs to know the index scale of the incident, as highlighted by Anucharan et al. (2025), the NBR has a high accuracy of 90.6% in identifying burned regions.

6. CONCLUSION

Integrating multi-spectral indices with geospatial analysis represents a significant advancement in the capacity to forecast and manage the risks associated with wildfires. This study has effectively developed an effective Fire Hazard Index (FHI) by integrating data from LST, NDVI, NDMI, NDWI, NDDI, and NBR. The FHI analyses both the environmental and meteorological factors that contribute to wildfire occurrence and successfully identifies the wildfire hazard zone within Perlis state. The findings highlight that the NBR and NDDI were the most significant influential factors of wildfire occurrence during the hot and dry weather. The FHI is a crucial instrument for decision-making as climate change increasingly induces prolonged dry seasons. It protects both natural ecosystems and human habitats from the devastating impacts of uncontrolled wildfires. This index also benefited local agencies, such as the Fire and Rescue departments, the Drainage and Irrigation Department, the State Forestry Department, and the Department of Environment.

Acknowledgments: Thank you to the Research and Industrial Linkages Division, Universiti Teknologi MARA Perlis Branch, which provided funding for graduate research assistance under Geran Semarak Penyelidikan - Penyeliaan (GSPP) with reference number UiTM.800-3/1 DDN.09 (017/2025).

References

Anucharan, T., Sroprom, T., Chaikaew, N., & Iamchuen, N. (2025). Assessing Burn Severity and Vegetation Impact Using Sentinel-2 Satellite Imagery and Geospatial Analysis in Mae Ka Subdistrict, Mueang District, Phayao, Thailand. *International Journal of Geoinformatics*, *21*(4), 51–70.

Artikanur, S., Widiatmaka, Setiawan, Y., & Marimin. (2022). Normalized Difference Drought Index (NDDI) computation for mapping drought severity in Bojonegoro Regency, East Java, Indonesia Normalized Difference Drought Index (NDDI) computation for mapping drought severity in Bojonegoro Regency, East Java, Indones. *Earth and Environmental Science*. https://doi.org/10.1088/1755-1315/1109/1/012027

Bandara, S., Navaratnam, S., & Rajeev, P. (2023). Bushfire Management Strategies: Current Practice, Technological Advancement and Challenges. *Fire*, *6*(11). https://doi.org/10.3390/fire6110421

Burapapol, K., & Nagasawa, R. (2016). Mapping Soil Moisture as an Indicator of Wildfire Risk Using Landsat 8 Images in Sri Lanna National Park, Northern Thailand. *Journal of Agricultural Science*, *8*(10), 107. https://doi.org/10.5539/jas.v8n10p107

Chew, Y. J., Ooi, S. Y., & Pang, Y. H. (2023). MCD64A1 Burnt Area Dataset Assessment using Sentinel-2 and Landsat-8 on Google Earth Engine: A Case Study in Rompin, Pahang in Malaysia. *13th IEEE Symposium on Computer Applications and Industrial Electronics, ISCAIE 2023*, 38–43. https://doi.org/10.1109/ISCAIE57739.2023.10165382

Chew, Y. J., Ooi, S. Y., Pang, Y. H., & Wong, K. S. (2022). A Review of Forest Fire Combating Efforts, Challenges and Future Directions in Peninsular Malaysia, Sabah, and Sarawak. *Forests*, *13*(9), 1–37. https://doi.org/10.3390/f13091405

Fisal, N. S. M., Lintangah, W., & Ismenyah, M. (2017). Community Awareness & Challenges in Forest Fire Prevention: a Case Study At Peat Swamp Forest, Klias Forest Reserve, Beaufort, Sabah, Malaysia. *International Journal of Agriculture, Forestry and Plantation*, *5*, 86–91.

Jamaruppin, M. E. Bin, Bayuaji, L., Ab Ghani, N. B., Rahman, M. A., Akashah, F. W., & Shah, A. (2016). Forest Fire Occurrence Analysis Base on Land Brightness Temperature using Landsat Data (Study Area: Jalan Kuantan–Pekan, Pahang, Malaysia). *The National Conference for Postgraduate Research*, 798–805.

Liu, D., & Zhang, Y. (2015). Research of regional forest fire prediction method based on multivariate linear regression. *International Journal of Smart Home*, *9*(1), 13–22. https://doi.org/10.14257/ijsh.2015.9.1.02

Moisa, M. B., Gabissa, B. T., Wedajo, Y. N., Gurmessa, M. M., Deribew, K. T., Negasa, G. G., Negassa, M. D., & Gemeda, D. O. (2023). Analyzing the correlation of forest and wetland with land surface temperature by using geospatial technology: a case of Yayo district, Southwestern Ethiopia. *Geocarto International*, *38*(1). https://doi.org/10.1080/10106049.2023.2256300

Nguyen, T. T. N., & Tong, T. H. (2023). Wildfire Risks In The Southwest Of Ky Son District , Nghe An Province – A Multi-Critical Model. *Journal of Science and Technique*, 7–18. https://doi.org/10.56651/lqdtu.jst.v6.n01.662.sce

Oliveira, S., Oehler, F., San-Miguel-Ayanz, J., Camia, A., & Pereira, J. M. C. (2012). Modeling spatial patterns of fire occurrence in Mediterranean Europe using Multiple Regression and Random Forest. *Forest Ecology and Management*, *275*, 117–129. https://doi.org/10.1016/j.foreco.2012.03.003

Rendana, M., Idris, W. M. R., Rahim, S. A., Abdo, H. G., Almohamad, H., Al Dughairi, A. A., & Albanai, J. A. (2023). Current and future land fire risk mapping in the southern region of Sumatra, Indonesia, using CMIP6 data and GIS analysis. *SN Applied Sciences*, *5*(8). https://doi.org/10.1007/s42452-023-05432-6

Thangavel, K., Spiller, D., Sabatini, R., Amici, S., Sasidharan, S. T., Fayek, H., & Marzocca, P. (2023). Autonomous Satellite Wildfire Detection Using Hyperspectral Imagery and Neural Networks: A Case Study on Australian Wildfire. *Remote Sensing*, *15*(3). https://doi.org/10.3390/rs15030720

Zahran, E. S. M. M., Shams, S., & Said, S. N. matullah B. M. (2020). Validation of forest fire hotspot analysis in GIS using forest fire contributory factors. *Systematic Reviews in Pharmacy*, *11*(12), 249–255. https://doi.org/10.31838/srp.2020.12.40